GSE statistics without spin

2014 EPL 107 50004

(http://iopscience.iop.org/0295-5075/107/5/50004)

A Letters Journal Exploring the Frontiers of Physics

September 2014

EPL, **107** (2014) 50004 www.epljournal.org
doi: 10.1209/0295-5075/107/50004

GSE statistics without spin

Christopher H. Joyner[1,2(a)], Sebastian Müller[2] and Martin Sieber[2]

[1] *Department of Physics of Complex Systems, The Weizmann Institute of Science - Rehovot 7610001, Israel*
[2] *School of Mathematics, University of Bristol - Bristol, BS8 1TW, UK*

received 13 June 2014; accepted in final form 11 August 2014
published online 27 August 2014

PACS 05.45.Mt – Quantum chaos; semiclassical methods
PACS 02.10.Ox – Combinatorics; graph theory
PACS 03.65.Fd – Algebraic methods

Abstract – Energy level statistics following the Gaussian Symplectic Ensemble (GSE) of Random Matrix Theory have been predicted theoretically and observed numerically in numerous quantum chaotic systems. However, in all these systems there has been one unifying feature: the combination of half-integer spin and time-reversal invariance. Here we provide an alternative mechanism for obtaining GSE statistics that is derived from geometric symmetries of a quantum system which alleviates the need for spin. As an example, we construct a quantum graph with a discrete symmetry given by the quaternion group $Q8$ and observe GSE statistics within one of its subspectra. We then show how to isolate this subspectrum and construct a quantum graph with a scalar valued wave function and a pure GSE spectrum.

Introduction. – In the 1950s and 1960s Wigner and Dyson pioneered the use of random matrices in modelling the statistical properties of the energy eigenvalues belonging to complicated quantum systems [1,2]. The techniques they developed spawned a new field of mathematics which has since become known as Random Matrix Theory (RMT) and its application has spread far and wide to many areas of mathematics and physics [3]. In particular it was later conjectured [4] that the high-lying quantum energy levels of classically chaotic systems are statistically distributed like eigenvalues of random matrices.

Central to the modelling of quantum systems by RMT is Dyson's *threefold way* [2], which groups quantum systems without geometric symmetries into three distinct types. The first occurs if time-reversal invariance is broken, for example by a magnetic field, meaning the quantum Hamiltonian H is inherently complex. The remaining two appear if there is an antiunitary time-reversal operator $\mathcal{T}$ which leaves H invariant, *i.e.* $[\mathcal{T}, H] = 0$. They are then distinguished by either $\mathcal{T}^2 = 1$ or $\mathcal{T}^2 = -1$, in which case H is real symmetric or quaternion-real, respectively. According to the aforementioned random matrix conjecture for chaotic systems [4], RMT makes predictions in all three instances by averaging over an ensemble of Hermitian matrices with the appropriate internal structure and Gaussian weighted elements. These are referred to as the Gaussian Unitary, Orthogonal and Symplectic Ensembles (GUE, GOE and GSE). We note that the number of symmetry classes can be extended to ten if additional anti-commuting symmetries are present [5,6] but this is beyond the scope of this letter.

In systems without geometrical symmetries time-reversal invariance with $\mathcal{T}^2 = -1$, and hence GSE statistics, have so far only been obtained in systems with wave functions that have an even number of components, commonly associated with half-integer spin. For such systems GSE statistics have been predicted and/or observed numerically in examples such as quantum billiards [7], maps [8] and quantum graphs [9], and explained using periodic-orbit theory [10,11]. However, to date there has been no experimental observation.

For systems with geometric symmetries the situation becomes more involved. Here the Hilbert space decomposes into subspaces invariant under symmetry transformations, and the spectral statistics inside these subspaces depends both on the system's behaviour under time reversal and on the nature of the subspace. For example 3-fold rotationally invariant chaotic quantum systems display GUE statistics within certain subspectra even if they are time-reversal invariant [12–14].

Remarkably, Dyson's formalism also permits GSE statistics in quantum systems without spin (by which

(a) E-mail: christopher.joyner@weizmann.ac.il

we mean systems with single-component wave functions), provided they have a certain kind of discrete symmetry. More precisely, this occurs within subspectra of systems with $\mathcal{T}^2 = 1$ that are associated to so-called pseudo-real irreducible representations of the symmetry group. Here we present an example of such a system – a quantum graph with a symmetry given by the quaternion group $Q8$. We then proceed to show how one can isolate this subspectrum and obtain a second quantum graph with scalar wave functions and a pure GSE spectrum. We note that pseudo-real irreducible representations can also arise in the context of cellular billiards [15].

Universality in subspectra. – Let us first recall some important concepts regarding discrete symmetries in quantum mechanics [16]. If g is a classical symmetry operation in, say, position space, a corresponding quantum-mechanical operator $U(g)$ can be defined by $U(g)\psi(\boldsymbol{r}) = \psi(g^{-1}(\boldsymbol{r}))$, and the Hamiltonian of the symmetric quantum system commutes with this operator. The unitary operators $U(g)$ form a representation of the symmetry group $\mathcal{G}$, *i.e.* they satisfy $U(g)U(g') = U(gg')$ for all $g, g' \in \mathcal{G}$. It can then be shown that the operators $U(g)$ have block-diagonal form in an appropriate basis of eigenfunctions of the Hamiltonian. The blocks correspond to irreducible representations (irreps) of the symmetry group. For finite groups there are only a finite number of irreps which we label by α and the corresponding block size is the dimension s_α of the irrep α. The s_α eigenfunctions corresponding to the same block are energy-degenerate. If we assemble them into an s_α-dimensional vector $|\alpha, n\rangle$, then the operators $U(g)$ act as

$$U(g)|\alpha, n\rangle = M^{(\alpha)}(g)^T|\alpha, n\rangle, \tag{1}$$

where n labels different blocks belonging to the same irrep α and $M^{(\alpha)}(g)$ is the matrix representing g in the irrep α. In this way the spectrum falls into subspectra associated to the different irreps. For example, in a system with mirror symmetry the symmetry group consists of the identity e and the reflection operator r. Then there are two one-dimensional irreps with $M^{(\pm)}(e) = 1$ and $M^{(\pm)}(r) = \pm 1$ corresponding to wave functions even and odd under reflection.

Like the behaviour under time reversal, all irreps may be classified into one of three types, depending on how they are related to their complex conjugate. Firstly if there does not exist a unitary matrix S such that

$$M^{(\alpha)}(g) = S^{-1}M^{(\alpha)}(g)^* S \quad \forall\, g \in \mathcal{G}, \tag{2}$$

then α is said to be *complex*. Alternatively if (2) holds and $S = S^T$, then α is *real* as all $M^{(\alpha)}(g)$ can simultaneously be made real by some unitary transformation. Whereas if (2) holds and $S = -S^T$, then an appropriate unitary transformation leads to a quaternion real form consisting of 2×2 blocks $\left(\begin{smallmatrix} a & b \\ -b^* & a^* \end{smallmatrix}\right)$ with $a, b \in \mathbb{C}$, and the representation is called *pseudo-real* (or quaternionic).

This classification is important as it defines which spectral statistics appear within each subspace [2]. Following Zirnbauer (Chapt. 3 of [3]), one can introduce a *transferred time-reversal* operator $\bar{\mathcal{T}} = Z\mathcal{T}$, where Z is unitary and $\mathcal{T}$ is the antiunitary symmetry of the full system. $\bar{\mathcal{T}}$ is obtained by ensuring that $|\alpha, n\rangle$ and $\bar{\mathcal{T}}|\alpha, n\rangle$ both transform in the same fashion under the action of $U(g)$, *i.e.* $U(g)\bar{\mathcal{T}}|\alpha, n\rangle = M^{(\alpha)}(g)^T\bar{\mathcal{T}}|\alpha, n\rangle$ is satisfied in addition to (1). If, for example, $\mathcal{T}$ is given by complex conjugation and α is either real or pseudo-real then one sees that $\bar{\mathcal{T}} = S\mathcal{T}$, with S as in (2), satisfies this requirement. One can show that $\bar{\mathcal{T}}$ is the correct antiunitary symmetry of the subspace associated to the irrep α [3]. It has the following interpretation: If the full system is desymmetrised in such a way as to isolate the subspace α, then $\bar{\mathcal{T}}$ becomes the only remaining symmetry of the system.

The type of spectral statistics within the subspace α depends only on this transferred time-reversal operator. In particular, if $\bar{\mathcal{T}}^2 = -1$, then one expects GSE statistics. This occurs if α is pseudo-real because then $\bar{\mathcal{T}}^2 = SS^*\mathcal{T}^2 = -\mathcal{T}^2 = -1$ (since $S = -S^T$). It also implies that $|\alpha, n\rangle$ and $\bar{\mathcal{T}}|\alpha, n\rangle$ are linearly independent, leading to Kramer's degeneracy [17].

The present argument for the appearance of GSE statistics relies purely on identifying the appropriate RMT symmetry class, in the spirit of [4]. However, one may extend semiclassical methods for systems without geometrical symmetries (see [18–20] and references therein) to explain why individual chaotic systems are faithful to these predictions [14,21]. This builds upon earlier semiclassical work by Keating and Robbins [13] who incidentally predicted that subspectra associated to pseudo-real irreps show GOE behaviour. However, they only investigated the so-called diagonal approximation, in which GOE is indistinguishable from GSE if one does not remove Kramer's degeneracy.

Quantum graphs. – To exemplify how pseudo-real subspaces can arise in systems without spin we turn to quantum graphs [22,23]. Quantum graphs consist of vertices v connected by one-dimensional bonds $b = (v_1, v_2)$. Each bond has a specified length L_b and the time-independent Schrödinger equation on each bond reads

$$H\psi(x) = -\frac{\mathrm{d}^2}{\mathrm{d}x^2}\psi(x) = E\psi(x), \tag{3}$$

where x defines the position on each bond. At the vertices the wave functions have to satisfy boundary conditions that make the Hamiltonian self-adjoint. For instance, one can consider Neumann (or Kirchhoff) boundary conditions; these require that at each vertex the wave functions of all adjacent bonds are equal and their outward pointing derivatives sum to zero.

We have chosen to use quantum graphs since their spectral statistics have been shown to agree with the corresponding random matrix predictions in the limit of large, sufficiently well-connected graphs [24,25] (assuming that

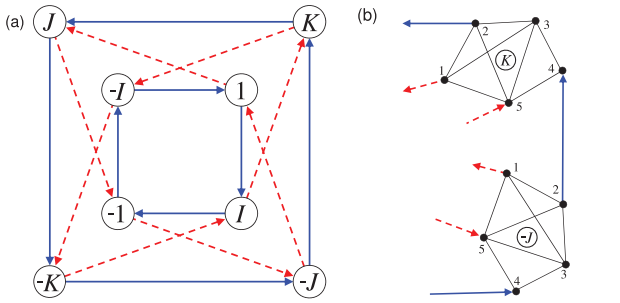

Fig. 1: (Colour on-line) (a) The Cayley graph of the quaternion group $Q8$ with solid (blue) bonds corresponding to the generator I and dashed (red) bonds to J; (b) an example subgraph being placed at the vertices $-J$ and K of the Cayley graph.

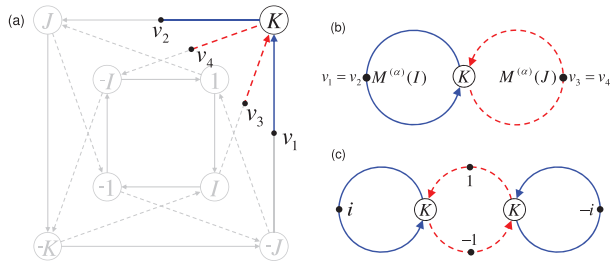

Fig. 2: (Colour on-line) (a) Definition of the points v_1, v_2, v_3, v_4 and the fundamental domain. The identification of the points v_1 with v_2 and v_3 with v_4 with vertex conditions as explained in the text leads either to (b) one copy of the fundamental domain with a two-component wave function or to (c) two copies with a one-component wave function.

the bond lengths are rationally independent). Moreover, in practice, numerical experiments agree well with RMT already for relatively small graphs [22].

All symmetry operations on a graph may be given in terms of permutations of the vertices. A permutation g is a symmetry if it leaves the connectivity and the bond lengths of the graph invariant, *i.e.*, if for every bond (v_1, v_2) there is a bond (gv_1, gv_2) and it has equal length.

In order to observe GSE statistics we must choose a discrete group which admits a pseudo-real irrep, the smallest and thereby easiest to construct is the quaternion group

$$Q8 := \{\pm 1, \pm I, \pm J, \pm K \colon I^2 = J^2 = K^2 = IJK = -1\}.$$

Here all group elements can be written as products involving two generators, for example I and J. One can show there are five irreps: Four real one-dimensional irreps given by $M(I) = \pm 1$, $M(J) = \pm 1$, and a fifth two-dimensional and pseudo-real irrep given by the quaternion-real matrices

$$M^{(5)}(I) = \begin{pmatrix} i & 0 \\ 0 & -i \end{pmatrix} \quad \text{and} \quad M^{(5)}(J) = \begin{pmatrix} 0 & 1 \\ -1 & 0 \end{pmatrix}. \quad (4)$$

One can verify the relation (2) is satisfied for this irrep with $S = M^{(5)}(J)$.

The aim is therefore to construct a quantum graph with this $Q8$ symmetry. Here we turn to a standard group-theoretical tool for visualising the structure of the group, known as the Cayley graph. Cayley graphs can be constructed for any discrete group by taking the group elements as vertices and connecting them by bonds related to the generators.

In the example of $Q8$, see fig. 1(a), we draw bonds between two vertices representing group elements if one element can be obtained from the other by *right multiplication* with either I or J. When interpreting the result as a quantum graph we choose the same length L_I for all bonds related to I and similarly L_J for J. The resulting graph is symmetric with respect to *left multiplication* of all elements in $Q8$. For example, let us consider a bond of length L_I given by $b = (g, gI)$, where $g \in Q8$, then application of any element $h \in Q8$ leads to the bond $b' = (hg, hgI) = (g', g'I)$ which is also a bond in our graph with length L_I.

However, at present our graph is still too small to be well described by random matrix theory. To obtain a larger graph which still retains the $Q8$ symmetry we can replace each of the vertices (corresponding to group elements) with identical subgraphs, see fig. 1(b). The connecting bonds (indicated by the arrows in fig. 1(a) and (b)) must then connect the vertices of the different subgraphs in a symmetric fashion. For larger subgraphs it is advisable to connect different subgraphs by more than one bond in order to obtain a well-connected graph that displays RMT statistics.

Now, importantly, our graph has subspectra associated to each of the irreps of $Q8$. This includes the four 1D irreps of degeneracy one and the remaining 2D, pseudo-real irrep of degeneracy four (two from the dimension of the representation and two from Kramer's degeneracy). The use of subgraphs serves to add complexity, meaning each subspectrum is expected to have RMT statistics. Remarkably this system consists entirely of *real scalar valued* wave functions and is capable of displaying GSE statistics – albeit within a particular subspectrum.

Quotient graphs. – In the following we show how to isolate this pseudo-real subspace, allowing us to construct a much smaller graph with a pure GSE spectrum. The methods for accomplishing this are detailed in [26,27], in which the authors define the concept of a "quotient graph". Here we describe two equivalent versions of this quotient graph, the first using a two-component wave function (fig. 2(b)), the second a (complex) scalar valued wave function (fig. 2(c)).

The general idea behind the first quotient graph is to use the eightfold symmetry to reduce the eigenfunctions to one eighth of the original graph (the fundamental domain). Equation (1) then dictates which boundary conditions are needed in order to select any particular irrep. We later show how the second version is obtained from the first.

We illustrate the construction of the quotient graph by starting from the Cayley graph with eight vertices, each representing one group element. One eighth of this graph will thus contain one vertex and half of each of the four generating bonds attached to it (see fig. 2(a)). For this we choose quite arbitrarily the vertex K and cut the bonds $(-J,K)$, (K,J), (I,K) and $(K,-I)$ in half at the points v_1, v_2, v_3, v_4. These points are related by symmetry operations, in particular the application of I takes the bond (K,J) to $(-J,K)$ and hence the point v_2 in the middle of the intervening bond to v_1. Similarly the application of J takes $(K,-I)$ to (I,K) and hence v_4 to v_3.

v_1, v_2, v_3, and v_4 now form the boundaries of the quotient graph and we have to identify boundary conditions that isolate the subspectrum associated to the pseudo-real representation. For this we combine the pairs of energy-degenerate eigenfunctions associated to this irrep into two-component wave functions $\boldsymbol{\psi}(x) = \langle x|\alpha, n\rangle$, where x denotes a position anywhere on the graph. The definition of $U(I)$ and the symmetries of the graph then imply $U(I)\boldsymbol{\psi}(v_1) = \boldsymbol{\psi}(I^{-1}v_1) = \boldsymbol{\psi}(v_2)$. Combining this with $U(I)\boldsymbol{\psi}(v_1) = M^{(5)}(I)^T\boldsymbol{\psi}(v_1)$ (see eq. (1)) we obtain

$$\boldsymbol{\psi}(v_2) = M^{(5)}(I)^T\boldsymbol{\psi}(v_1). \tag{5}$$

A similar result holds for the first derivatives if we let the coordinates along the bonds increase in the directions indicated by arrows in fig. 2. In this case we obtain a relation as in (5) also for points moved compared to v_1 and v_2 by the same amount, and differentiating with respect to this amount yields

$$\boldsymbol{\psi}'(v_2) = M^{(5)}(I)^T\boldsymbol{\psi}'(v_1). \tag{6}$$

Analogous reasoning for the points v_3 and v_4 gives the conditions

$$\boldsymbol{\psi}(v_4) = M^{(5)}(J)^T\boldsymbol{\psi}(v_3), \tag{7}$$
$$\boldsymbol{\psi}'(v_4) = M^{(5)}(J)^T\boldsymbol{\psi}'(v_3). \tag{8}$$

Hence we identify v_1 with v_2 and v_3 with v_4 up to multiplication of $\boldsymbol{\psi}$ with a matrix, see fig. 2(b). The relations (5) to (8) have the effect of isolating the pseudo-real representation, now with two-component eigenfunctions supported on one eighth of the original graph.

Now, crucially, an equivalent form of the quotient graph can be realized using only scalar wave functions. This is achieved by taking the two components of $\boldsymbol{\psi}$ to reside on two different copies of the graph. Equations (4) and (5) then imply that on the first copy $\psi_1(v_1) = i\psi_1(v_2)$ and on the second $\psi_2(v_1) = -i\psi_2(v_2)$, with analogous relations for the derivatives (eq. (6)). In contrast, eq. (7) and the off-diagonal form of $M^{(5)}(J)$ in (4), imply that the two subgraphs are joined at the two copies of v_3 and v_4, with the conditions $\psi_1(v_4) = -\psi_2(v_3)$ and $\psi_2(v_4) = \psi_1(v_3)$, as illustrated in fig. 2(c). Combining the two copies thus leads to a graph with a single-component wave function $\psi(x)$.

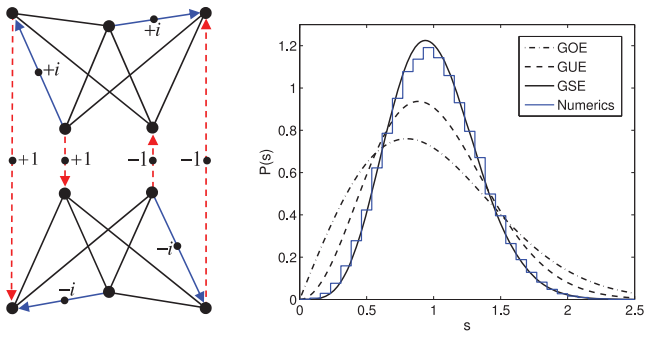

Fig. 3: (Colour on-line) (a) Quotient graph containing bonds with appropriate complex phase factors $\pm i$ and ± 1. (b) Nearest-neighbour spacing distribution, averaged over 10 graphs with 10000 energy levels each.

In this form, the quotient graph possesses a very intriguing antiunitary symmetry, derived from the operator $\bar{\mathcal{T}} = S\mathcal{T}$, introduced earlier. In the present context it has the action $\bar{\mathcal{T}}\psi(x_{1/2}) = \pm\psi^*(x_{2/1})$, where $x_{1/2}$ denotes x in the first/second copy of the graph. $\bar{\mathcal{T}}$ thus serves to exchange the wave function on each copy with the complex conjugated wave function from the opposing copy, but does so with different signs. The presence of this antiunitary symmetry, satisfying $\bar{\mathcal{T}}^2 = -1$, provides an alternative explanation for the appearance of GSE statistics, that is independent of our group theoretical arguments above. It furthermore leads to a Kramer's degeneracy in the spectrum of the quotient graph.

Finally, we note the discontinuities at the vertices v_1, v_2, v_3, v_4 can be avoided by introducing magnetic fluxes A along the bonds instead, which might be relevant for an experimental realisation. This requires modifying the Hamiltonian (3) to $(-i\mathrm{d}/\mathrm{d}x + A)^2$ [23]. If A is chosen appropriately, this generates the same phases as the discontinuous vertex conditions (5)–(8), but spread along the bonds rather than at a single point. A gauge invariance principle then guarantees that the spectrum remains the same.

For a numerical check we calculated the spectrum of the quotient graph displayed in fig. 3(a). We took an average over ten random realisations with bond lengths distributed uniformly between 0 and 1. Figure 3(b) shows a good agreement with Wigner's GSE prediction [1,17] for the distribution $P(s)$ of spacings s between neighbouring energy levels (normalized to yield an average spacing of 1). The distribution of each individual realisation differs only slightly from the mean. The choice of two bonds with I and J conditions corresponds to a better connectivity in the full $Q8$-symmetric graph than with only one bond, as mentioned earlier. We also investigated larger graphs and found that we obtain better agreement with RMT if they are sufficiently well connected. This is similar to the case of non-symmetric graphs.

Conclusions. – In summary, we have given theoretical arguments and provided numerical evidence that GSE statistics can be observed in systems without spin – utilizing the pseudo-real irrep of $Q8$ to construct a spinless quantum system with an anitunitary operator squaring to -1. We note that current techniques allow quantum graphs to be manufactured to within tolerances where the effects of symmetries can be successfully observed [28]. Therefore, quantum graphs, in the form proposed here, and, *e.g.*, built using optical fibres or coaxial cables [29], offer the possibility of a first experimental observation of GSE statistics. It would also be interesting to identify further experimental realisations of symmetries with pseudo-real representations and investigate geometrical symmetries within the framework of the new symmetry classes [5,6].

* * *

The authors are indebted to R. Band for all the help and guidance received during this work. We would also like to thank J. Harrison and U. Smilansky for useful advice.

REFERENCES

[1] Wigner E. P., *Ann. Math.*, **62** (1955) 548.
[2] Dyson F. J., *J. Math. Phys.*, **3** (1962) 1199.
[3] Akemann G., Baik J. and Francesco P. D. (Editors), *The Oxford Handbook of Random Matrix Theory* (Oxford University Press) 2011.
[4] Bohigas O., Giannoni M. J. and Schmit C., *Phys. Rev. Lett.*, **52** (1984) 1.
[5] Zirnbauer M. R., *J. Math. Phys.*, **37** (1996) 4986.
[6] Altland A. and Zirnbauer M. R., *Phys. Rev. B*, **55** (1997) 1142.
[7] Berry M. V. and Mondragon R. J., *Proc. R. Soc. Lond. A*, **412** (1987) 53.
[8] Keppeler S., Marklof J. and Mezzadri F., *Nonlinearity*, **14** (2001) 719.
[9] Bolte J. and Harrison J., *J. Phys. A: Math. Gen.*, **36** (2003) 2747.
[10] Bolte J. and Harrison J., *J. Phys. A: Math. Gen.*, **36** (2003) L433.
[11] Braun P., *J. Phys. A: Math. Theor.*, **45** (2012) 045102.
[12] Leyvraz F., Schmit C. and Seligman T. H., *J. Phys. A: Math. Gen.*, **29** (1996) L575.
[13] Keating J. P. and Robbins J. M., *J. Phys. A: Math. Gen.*, **30** (1997) L177.
[14] Joyner C. H., Müller S. and Sieber M., *J. Phys. A: Math. Theor.*, **45** (2012) 205102.
[15] Gutkin B., *Nonlinearity*, **24** (2011) 1743.
[16] Elliot J. P. and Dawber P. G., *Symmetry in Physics*, Vol. **1** (Macmillan, Basingstoke) 1979.
[17] Haake F., *Quantum Signatures of Chaos*, 3rd edition (Springer, Heidelberg) 2010.
[18] Berry M. V., *Proc. R. Soc. Lond. A*, **400** (1985) 229.
[19] Sieber M. and Richter K., *Phys. Scr.*, **T90** (2001) 128.
[20] Müller S., Heusler S., Altland A., Braun P. and Haake F., *New J. Phys.*, **11** (2009) 103025.
[21] Joyner C. H., PhD Thesis, University of Bristol (2012).
[22] Kottos T. and Smilansky U., *Ann. Phys. (N.Y.)*, **274** (1999) 76.
[23] Gnutzmann S. and Smilansky U., *Adv. Phys.*, **55** (2006) 527.
[24] Gnutzmann S. and Altland A., *Phys. Rev. Lett.*, **93** (2004) 194101.
[25] Berkolaiko G., *Form factor expansion for large graphs: a diagrammatic approach*, in *Quantum Graphs and Their Applications*, edited by Berkolaiko G., Carlson R., Fulling S. A. and Kuchment P., *Contemporary Mathematics*, Vol. **415** (AMS, Providence, RI) 2006, p. 35.
[26] Band R., Parzanchevski O. and Ben-Shach G., *J. Phys. A: Math. Theor.*, **42** (2009) 175202.
[27] Parzanchevski O. and Band R., *J. Geom. Anal.*, **20** (2010) 439.
[28] Hul O., Ławniczak M., Bauch S., Sawicki A., Kuś M. and Sirko L., *Phys. Rev. Lett.*, **109** (2012) 040402.
[29] Hul O., Bauch S., Pakoński P., Savytskyy N., Życzkowski K. and Sirko L., *Phys. Rev. E*, **69** (2004) 056205.